NUMERICAL SIMULATION STUDY ON THE EFFECTS OF FOUNTAIN ON AROUND THERMAL ENVIRONMENT

Borong Lin[1], Zhiqin Zhang[2], Xiaofeng Li[1,] Yingxin Zhu[1]

[1]Department of Building Science and Technology, Tsinghua University, Beijing, 100084, China
[2] Department of Mechanical Engineering, Texas A&M University, USA

ABSTRACT

With the fast development of urbanization in China, the urban thermal environment has been worsen due to the more and more obvious heat island phenomena. Aartificial waterscape is regarded as one of the most effective methods to improve the outdoor climate. In this paper a fountain model is developped based on experiment results and Particle-Source-In Cell (PSI-CELL) model. Lagrangian approach is adopted to simulate the dynamics properties of droplets in the air while Eulerian approach is employed to solve the conservation equations of the air. The droplet size and velocity distributions are calculated based on the atomization property of the pressure pipe nozzle. The predicted results have been compared against the experiment values. The resulting inaccuracy can be traced back to the change of prevailing wind direction and velocity changes as also as the atomization analysis. Finally the affected factors have been discussed.

KEYWORDS

Outdoor thermal environment, fountain, PSI-CELL model, Lagrangian approach, Droplet

INTRODUCTION

In recent years, increasing industrialization and urbanization are significantly affecting the urban climate in China. The poor effects of heat island is more and more obvious. Aartificial waterscape, such as pool, fountain, and canal, is regarded as one of the most effective methods to improve the outdoor climate and people began to study its performance more quantitively. In this paper a fountain model is developped based on experiment results and PSI-CELL model[1], which is dealt with the process of two-way coupling between air and droplet. And Lagrangian approach is adopted to simulate the dynamics properties of droplets in the air while Eulerian approach is employed to solve the conservation equations of the air.

MODEL FORMULATION

Heat and mass transfer between droplets and air

The fundamental process is the heat and mass transfer between droplets and air, which has been extensively investigated. A quasi-stable evaporation state needs to be considered, which is found to be accurate enough[2]. Based on these assumptions, the droplet diameter formula can be described by [3]:

$$\frac{d\left(D_p^2\right)}{dt} = \frac{-4\rho_g D_c \mathrm{Nu} \ln\left(1+B_M\right)}{\rho_p} \qquad (1)$$

According to the energy conservation equation, droplet temperature can be calculated by:

$$\frac{dT_p}{dt} = AT_a - BT_p + C \qquad (2)$$

If performing integration on equation (1) and equation (2), the droplet temperature and diameter change along the trajectory can be figured out.

Dynamics of droplets in air

In Lagrangian approach, droplet velocity can be calculated by dynamic analysis and then the trajectory can be calculated by performing integration on droplet's velocity. Due to the quite large particle-fluid density ratio, dominant forces in the droplet motion equation are reduced to air drag force

and gravity force, leading to:

$$m_p \frac{d\vec{U}_p}{dt} = Dr_p(\vec{U} - \vec{U}_p) + m_p \vec{g} \quad (3)$$

Since the droplet is treated as a separate stiff sphere, the drag function Dr_p is:

$$Dr_p = \frac{1}{2}\rho A_P C_D \left|\vec{U} - \overrightarrow{U_P}\right| \quad (4)$$

Especially, A_p is the projection area of a droplet. Drag coefficient C_D is given by the following formula [4]:

$$\text{Re}\leq 1000,\quad C_D = \frac{24(1+0.15\,\text{Re}^{0.687})}{\text{Re}}$$
$$\text{Re}>1000,\quad C_D = 0.44 \quad (5)$$

When droplet velocity is obtained from equation (3), the droplet trajectory can be yielded by integrating following equation:

$$\frac{d\vec{x}_p}{dt} = \vec{U}_p \quad (6)$$

In Lagrangian approach, an optional stochastic turbulence model is adopted to account for the effects on particle dispersion of the turbulent fluctuations of the continuous-phase velocity. This method came from Gosman, Ioannides[5] and Shuen, etc.[6, 7].

PSI-CELL model

In this research, two-way coupling between air and droplet is simulated by Particle-Source-In Cell (PSI-CELL) mode, which is firstly raised by Migdal and Agosta[1]. The main idea is to treat the effects of droplet to air as the source items in mass, momentum, and energy equations of air phase. The airflow field is simulated by solving differential equations with Eulerian approach. The droplet is traced along its trajectory according to Lagrangian approach. Its temperature and diameter can be calculated by performing integration on the dynamic equation.

The continuous phase is simulated by Eulerian equation as following:

$$\frac{\partial}{\partial t}(\rho_c \phi_c) + \nabla\cdot(\vec{U}_c \rho_c \phi_c) - \nabla\cdot(\Gamma \nabla \phi_c) = S_\phi + S_{\phi G} \quad (7)$$

When droplets move across a cell, the mass source S_m, momentum source S_{mom} and the energy source S_h can be calculated by:

$$S_m = \frac{\pi}{6}\sum \eta\left[\rho_p^o \left(D_p^o\right)^3 - \rho_p^n \left(D_p^n\right)^3\right] \quad (8)$$

$$S_{mom} = \frac{\pi}{6}\sum \eta\left[\rho_p^o U_p^o \left(D_p^o\right)^3 - \rho_p^n U_p^n \left(D_p^n\right)^3\right] \quad (9)$$

$$S_h = \frac{\pi}{6}\sum \eta\left[\rho_p^o h_p^o \left(D_p^o\right)^3 - \rho_p^n h_p^n \left(D_p^n\right)^3\right] \quad (10)$$

Firstly, the initial flow field is calculated discarding droplets and then the trajectory, diameter and temperature change of the droplets can be counted. With these data, the mass, momentum, and energy source items of the droplets in every cell can be obtained. Then these source items are added to the corresponding conservation equations and new airflow field can be obtained. The new flow field is used to calculate the new trajectory, diameter and temperature of the droplets. Therefore, the coupling effect between air and droplet is considered. The procedure above is repeated until the droplet disappeared in the field.

Initial diameter and velocity profiles of droplets

In heat and mass transfer process between droplets and air, droplet mean diameter and diameter profile are most important parameters, which are determined by many factors, such as nozzle property and liquid properties. Since it is difficult to describe the droplet diameter and its velocity one by one, distribution function is an efficient means to describe these parameters. Because the mechanism analysis on droplet diameter distribution is lack, some functions based on probability or pure experiences have been concluded, such as normal, log-normal, Nukiyama-Tanasawa, Rosin-Rammler, and Upper-limit distribution [8].

The spray velocity distribution is another important parameter. Sellens and Brzustowski[9] obtained the droplet diameter and velocity distribution function of rotary pressure nozzle according to maximum entropy principle and fundamental physical conservation laws. For fixed diameter, the velocity profile agrees normal distribution. Some practical

data revealed that the droplet dimensionless velocity range is 0.5~1.5[10]. The droplet velocity near the nozzle will reach a homogenous distribution under the air current affect. It is reasonable to assume the same initial velocity for the same size droplets. Therefore, an equal initial velocity is adopted for the same size droplets.

Jet breakup

Besides what have been discussed above, the process of the jet breakup needs to be considered, which decides droplet size and velocity distribution.

Research discovered that the droplet size distribution of the first and second breakup fitted the universal root normal distribution with MMD/SMD equaled to 1.2. Therefore, the droplet size after the second breakup can be calculated with SMD [11]. Experiment result found that the final droplet SMD could be yielded by:

$$\frac{\rho_G SMD u_o^2}{\sigma} = 12.9\left(\frac{x}{\Lambda}\right)^{1/3}\left(\frac{\rho_G}{\rho_L}\right)^{3/4} We_{L\Lambda}^{5/6}\,\mathrm{Re}_{L\Lambda}^{-1/2} \tag{11}$$

Where Λ is the radial integration size and it is D/8 for full development turbulent pipe flow[12]. $We_{L\Lambda} = \rho_L \bar{u}_o^2 \Lambda / \sigma$.

The volume-based distribution formula is:

$$\frac{dV}{dD} = f\left(V_{D_i}\right) = \frac{1}{\sqrt{2\pi}s_n}\exp\left[-\frac{1}{2s_n^2}\left(\sqrt{\frac{D_i}{D_{MMD}}}-1\right)^2\right] \tag{12}$$

Where S_n equal to 0.238. In $|3S_n|$ range or $0.082 < D_i/D_{MMD} < 2.938$, 99.74% of total water volume is included and it is precise enough to adopt this interval as the droplet size distribution range. The droplet velocity along the jet direction and vertical direction can be:

$$\frac{\tilde{u}_p}{\bar{u}_o} = 0.9 \qquad \frac{\tilde{v}_p}{\bar{u}_o} = 0.06 \tag{13}$$

FOUNTAIN EXPERIMENTS AND SIMULATION

Experiment introduction

A field experiment is conducted in Beijing in August to validate above theoretical model. The experiment field and measuring position are shown in Fig. 1 and Fig. 2. There are 13 measure points arranged around the fountain. The points are numbered according to its direction and distance related to the fountain. For example, N represents the points in the north part of the fountain and NW presents the points in the northwest part. Number 1 represents the nearest point and 4 presents the furthest point. On the south part of the fountain is the weather monitoring point.

In the field there are 12 points with dry bulb temperature (DBT) measurement and 8 points with Black Bulb Temperature (BBT) and relative humidity (RH) measurement. On the south part is the point of local weather conditions measurement. Besides, a sensor is put in a nozzle to obtain spray water temperature. All the sensors are synchronized and the data are reserved. The experiment started at 12:30 and ended at 17:00. After the experiment the data are output to computer to be treated and analyzed.

Simulation model

Simulation is performed using a commercial CFD code, which employs a standard finite volume method. This code has been validated in numerous applications that included cases with two-phase flow. The equations solved here are Reynolds-averaged Navier-Stokes equations, which predict average velocities, temperatures, and humidity for turbulent flows. k-ε Low Reynolds turbulence model was chosen for this study. The simulation zone size is 80m (L) × 47.5m (W) × 20m(H) and the grid number is 63 × 20 × 22. The property formulas of air, water, and vapor are added into the code. Evaporating droplet with stochastic turbulence model is used and droplet rebound and breakup on the ground are not considered.

Figure 1. Experiment field view

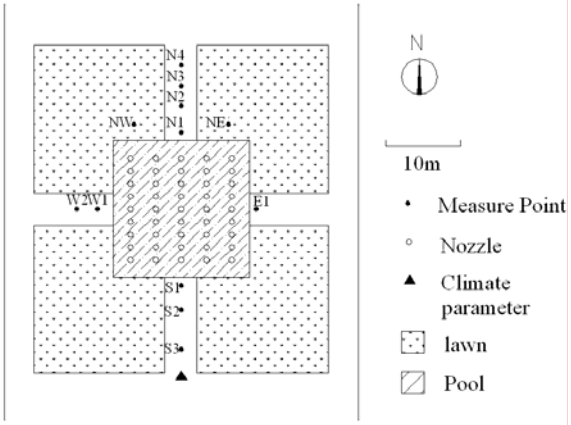

Figure 2. Measuring points layout

Boundary conditions

On the south and north of the fountain is meadow and on the east and west side are buildings. Because the affect of solar radiation and long wave radiation from the surrounding objects to the droplet is very small, radiation heat transfer is ignored and the ground around the fountain is supposed to be an underlying surface with the same property.

Part experiment results are used as the time independent input data for the simulations. During the experiment the prevailing direction is south with a little southern or western deviation occasionally. It brings much fluctuation of the thermal parameters in the leeward area. Accordingly, a period with stable prevailing direction is selected as the simulation object, which is from 12:30 to 13:30. To verify the effect of the prevailing direction on the thermal environment, simulation is also performed under SE, SSE, SSW, and SW prevailing direction. As the experiment data indicate, the average prevailing dry bulb temperature is 32.7℃ and the average moisture content is 14.9g/kg air. The relative humidity is 47.5% and it is hot. In the model the water temperature is set 24.5℃.

Wind speed varies with height above ground level. This is because friction at ground level slows the air down. In build-up areas, this boundary layer effect is greater owing to the rough surface created by large expanses of buildings. As a result, gradient wind profile is introduced. During the experiment, the prevailing velocity is measured 6m above the ground. The wind velocity fluctuates heavily and the average is 2.9m/s. Because the wind velocity has a significant affect on the thermal environment field, the measured data are cataloged into five zones, which are 0.0~1.2, 1.2~2.2, 2.2~3.7, 3.7~5.25 and 5.25~8.0 respectively. The average value in each zone is 0.9, 1.5, 2.9, 4.5 and 6.0, which will be set as the prevailing velocity 6m above the ground.

The initial jet velocity at the nozzle orifice is estimated according to the spray height of the jet. Since the velocity of large droplet is almost equal to the initial jet velocity and gravity is the only factor that may affect its dynamic trajectory, the velocity can be calculated from spray height, which is about 3.75m. The result is about 9.4m/s.

At the same time, formula (12) can be used to calculate the volume-based distribution of the droplets and then the mass-based and number-based distribution can be obtained. Based on the analysis above, the droplet diameter rang is set from 0.082MMD to 2.938MMD. The jet spouts out and then falls all around. Here it is simplified as four normal directions. All the droplets in one direction are divided into five zones according to its diameter. The average diameter, total mass, and total droplet number in each zone are calculated. To analysis the zone number independence on the simulation result, a simulation is carried out based on 10 zones. Little change is found in result comparing.

RESULTS AND DISCUSSION

Simulation results

As discussed previously, thermal environment around

a fountain is simulated under different wind velocity and direction. Because of space limited, only one typical scenario is showed in this paper while wind direction is normal south and the velocity is 2.9m/s. Normally, the outdoor environment is assessed at occupied zone, or a horizontal level 1.5m above the ground. Fig. 3-a~3-c show the isolines of difference value ΔDBT, ΔRH, and Δd, which equal to space value minus prevailing value. Fig. 3-d shows the vector field around the fountain. It can be found that fountain can evidently cool the leeward area, where ΔDBT is about -1.0~-4.0℃ and the maximum is -6.0 ℃. Especially -2.5℃ temperature drop is expected at 30m far away from the fountain. It is due to evaporation cooling of droplets. Accordingly, humidification effect is obvious in this area. ΔRH range is 5%~25% and 35% at some place. But the air is still not saturated. Moisture content change can more clearly explain this point. Δd is normally between 1.0 and 3.0g/kg dry air. The vector field shows that wind velocity decreases little on the leeward side. Simulation results verified the cooling and humidifying effect of the fountain on the leeward area but the wind field change is almost negligible.

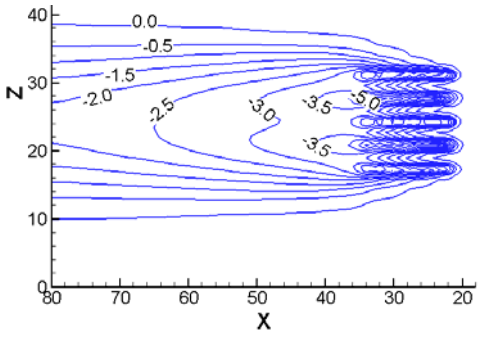

(a)ΔDBT

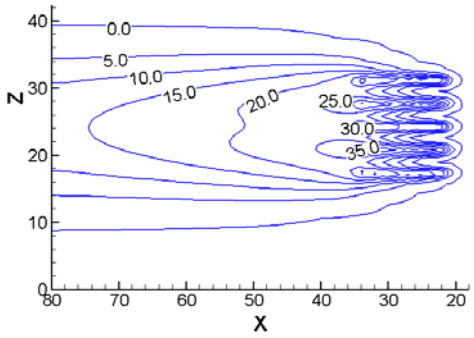

(b)ΔRH

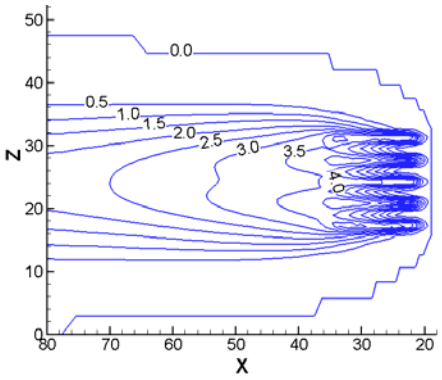

(c)Δd

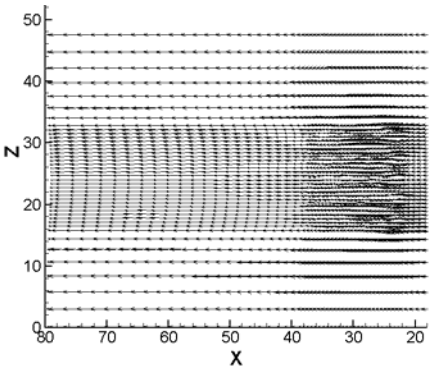

(d) $\vec{V}$

Figure. 3 Contour of thermal parameters at 1.5m horizontal level around the fountain

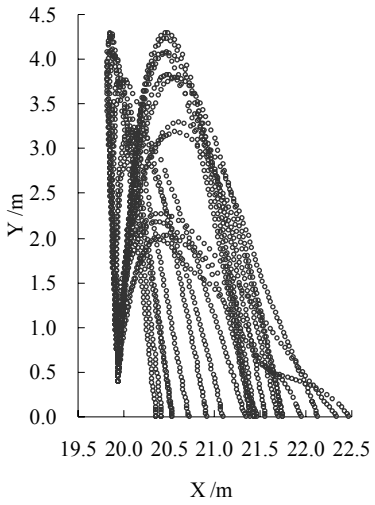

(a)Elevation view

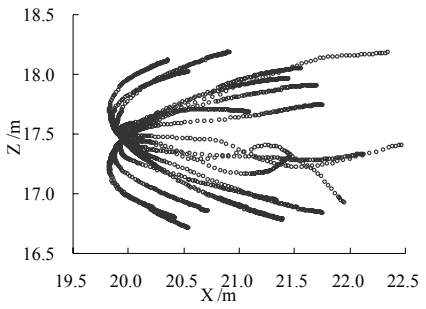

(b)Plan view

Figure.4 Droplets trajectories of the fountains

Figure 4 is the elevation view and plan view of the droplet trajectories spouting out from one nozzle. There are totally 20 bands of sprays, which eject in four directions. For larger droplets, the highest elevation is about 4.2m because of small air drag force. However, the range is only about 1.5m. In contrast, the smaller droplets affect heavily by the air drag force and float as far as 2.5m away from the nozzle. As stochastic turbulence model is adopted in the simulation, the trajectories of small droplets are random. All these feathers are verified in the experiment.

Comparing with experiment

During the experiment, the climate parameters changed continuously including prevailing velocity, direction, DBT, and RH. Simulation results indicate that the wind velocity and direction change has great effect on the field distribution while DBT and RH change may change the field value. Therefore, simulations are firstly carried out under different wind velocity and then different wind direction is considered. At last weighting method based on probability theory is used to yield the final result.

Firstly, the representative velocity is 0.9, 1.5, 2.9, 4.5, and 6.0 m/s. Experiment measures show that the probability p_i of every representative velocity is about 0.075, 0.255, 0.413, 0.191, and 0.066. Under different wind velocity the DBT or RH at one point are predicted. At last, the simulation result under south wind direction can be calculated by:

$$V_j = \sum_{i=1}^{5} p_i V_{j,i} \qquad (14)$$

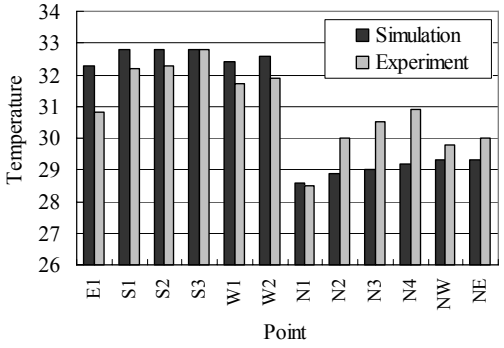

(a)DBT

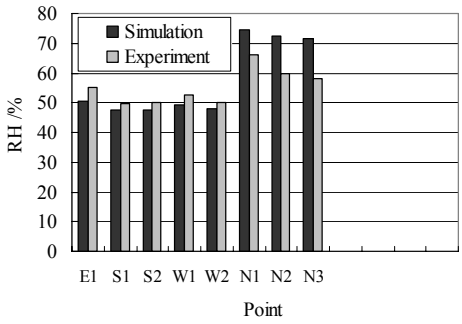

(b)RH

Figure 5 Comparing of simulation and experiment results(Direction is unconsidered)

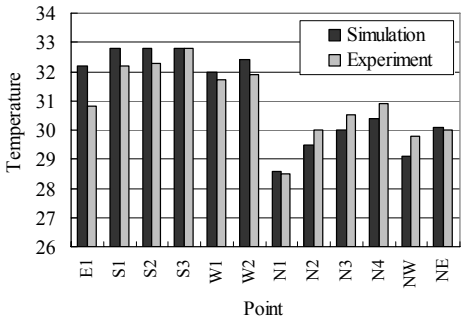

(a)DBT

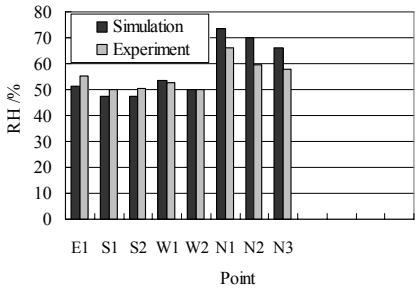

(b)RH

Figure 6 Comparing of simulation and experiment results(Direction is considered)

Figure 5-a shows the comparison of DBT and RH between simulation result and experiment result. It can be found that, for the points in the windward area or beside area, such as point E1, S1, W1 and W2, the absolute error is small because the fountain can only affect these areas lightly. However, the wind direction changed continuously and the simulation data are a little higher than the experiment result. The point E1 and W1 is just beside the fountain and the wind change can lead to large temperature fluctuation. Therefore, the simulation result is higher than the experiment result. For the points in the leeward area, the two results are also equal. But the deviations are almost larger than 1.1℃. Because the wind direction change will increase the temperature at these points and the wind direction effect should be considered. Figure 5-b is the relative humidity result and the simulation result in the windward area and the side area is 3.6% lower than the experiment result. In contrast, on the leeward side the simulation result is 12% higher than the experiment result because of wind direction fluctuation. Since a steady scenario is assumed, the prevailing direction change should be considered to minimize the error.

The prevailing wind directions can be classified as SE, SSE, S, SSW, and SW. According to the experiment record, the probability of different wind direction is about 0.15, 0.2, 0.5, 0.1 and 0.05. The wind velocity is set 2.9m/s and simulation is carried under different wind direction. The result at every point under different wind velocity is weighed with the wind direction probability. The final results are given in Figure 6-a and 6-b. It can be found that the absolute error of all points is within 0.7℃ except point E1 and the absolute error of majority points is below 5%.

CONCLUSION

The interaction between fountain and air is a complex process. The basis mechanism includes heat and mass transfer between droplet and air, droplet projectile motion in the air, two-phase flow with coupling effect, and jet breakup analysis. In this paper, all aspects have been used to develop a fountain model for predicting its effects on around thermal environment. At the same time, part experiment result is used as the time independent input data for the simulations. The simulation result is presented and the field data is compared with experiment data. It can be found that prevailing direction is a key factor on outdoor thermal environment. Not until this factor is considered based on probability method can the simulation result reasonably agree with the experiment result. Besides, Initial distributions of droplet size and velocity are another important parameter in the model, which are determined by nozzle property and liquid properties.

Due to the multiplicity of the fountain configurations and the complexity of the dynamic phenomena involved in jet breakup, the thermal performance of a fountain must be the object of extensive studies. This research is only one stage for better understanding of a particular type of fountain. In any case, these results cannot be generalized for other configurations of fountain and cannot be enough for the technical design of a fountain.

REFERENCE

Migdal, D., Agosta, V. D.. A source flow model for continuous gas-particle flow. J. Applied Mechanical, 1967, Vol. 35, No. 4, 860

H. Lefebvre. Atomization and sprays. Hemisphere publishing corporation, 1989, P310.

Chin, J. S., Lefebvre, A. H. Steady-state Evaporation Characteristics of Hydrocarbon Fuel Drops. AIAA J., Vol. 21, No. 10, 1986. 1437~1443

Wallis, G. B., One-Dimensional two-phase flow. Mcgraw Hill, New York, 1969

D. Gosman, E. Ioannides. Aspects of computer simulation of liquid fueled combustors, AIAA , 1986, paper 81-0323

J.-S. Shuen, A. S. P. Soloman, Q. -F. Zhang, G. M. Faeth. Structure of particle-laden jets: measurements and predictions. AIAA J.23, 1985, 396~404

Gauvin, W. H. Katta, S., Knelman, F. H.. Drop trajectory predictions and their importance in the design of spray dryers. Int. J. Multiphase Flow, 1975, Vol.1, 793

Mugele, R., Evans, H. D. Droplet size distribution in sprays, Ind. Eng. Chem., Vol. 43, No. 6, 1951, pp. 1317~1324

Sullens R. W., Brzustowski T. A. A simplified prediction of droplet velocity distributions in a sprays. Combustion and flame, vol. 65, 273~279

S. S. Kachhwaha, P. L. Dhar, S. R. Kale. Experimental studies and numerical simulation of evaporative cooling of air with a water spray-I. Horizontal parallel flow. Int. J. Heat Mass Transfer, 1998, 41(2): 447~464

Simmons, H. C. The correlation of drop-size distribution in fuel nozzle sprays. J. Engng Power, 1977, V99, pp. 309-319

J. O. Hinze. Turbulence, 2nd ed. ~McGraw-Hill, New York, 1975, pp. 427 and 724–742.

Nomenclature

A	area, m^2
C_D	drag coefficient
Cp	heat capacity, J/kg•K
d	Moisture content, g/kg dry air
D	diameter, m
Dc	mass diffusion rate, m^2/s
Dr	drag function
D_{30}	volume-based average diameter, m
D_{32}	Sauter average diameter, m
G	gravity acceleration, $9.8m/s^2$
H	enthalpy, J
k	turbulent energy, m^2/s^2
l	length, m
L	latent heat of vaporization, J/kg
m	mass, kg
n	droplet number
P	pressure, Pa, or probability
r	droplet radius, m
t	time, s
T	temperature, K
U	velocity, m/s
V	volume, m^3

Dimensionless number

B_M	mass transfer number
Nu	Nusselt number
Oh	Ohnesorge number
Pr	Prandtl number
Re	Reynolds number
We	Weber number

Greek letter

σ	standard deviation
ρ	density, kg/m^3
ε	turbulent kinetic dissipation rate, m^2/s^3
Γ	gamma function
Λ	radial integration size, m
Δ	difference
η	number of droplet beam

Suffix

a	air
c	continuous phase
g	mixture gas
G	source item
h	enthalpy
m	mass
max	maximum value
min	minimum value
mom	momentum
p	droplet
s	droplet surface
v	vapor
∞	infinite distance

Abbreviation:

CFD	Computational Fluid Dynamics
DBT	Dry Bulb Temperature
MMD	Mass Mean Diameter
PSI-CELL	Particle-Source-In Cell
RH	Relative humidity
SMD	Sauter Mean Diameter